Novel Humanized Monoclonal Antibodies for Targeting Hypoxic Human Tumors via Two Distinct Extracellular Domains of Carbonic Anhydrase IX

Miriam Zatovicova
MABPRO, a.s.; Institute of Virology, Biomedical Research Center Slovak Academy of Sciences: Biomedicinske centrum Slovenskej akademie vied

Ivana Kajanova
Institute of Virology SAS: Biomedicinske centrum Slovenskej akademie vied

Monika Barathova
MABPRO, a.s.; Institute of Virology, Biomedical Research Center Slovak Academy of Sciences: Biomedicinske centrum Slovenskej akademie vied

Martina Takacova
Institute of Virology SAS: Biomedicinske centrum Slovenskej akademie vied

Martina Labudova
MABPRO, a.s.; Institute of Virology SAS: Biomedicinske centrum Slovenskej akademie vied

Lucia Csaderova
Institute of Virology SAS: Biomedicinske centrum Slovenskej akademie vied

Lenka Jelenska
Institute of Virology SAS: Biomedicinske centrum Slovenskej akademie vied

Eliska Svastova
Institute of Virology SAS: Biomedicinske centrum Slovenskej akademie vied

Silvia Pastorekova
Institute of Virology SAS: Biomedicinske centrum Slovenskej akademie vied

Adrian L Harris
University of Oxford Department of Oncology

Jaromír Pastorek (jaromir.pastorek@mabpro.sk)
MABPRO, a.s. https://orcid.org/0000-0003-2163-0864

Research

Keywords: carbonic anhydrase IX, hypoxia, humanized antibody, tumor microenvironment

Posted Date: August 30th, 2021

DOI: https://doi.org/10.21203/rs.3.rs-827745/v1

Version of Record: A version of this preprint was published at Cancer & Metabolism on February 2nd, 2022. See the published version at https://doi.org/10.1186/s40170-022-00279-8.

Abstract

Background

Hypoxia in the tumor microenvironment (TME) is often the main factor in the cancer progression. Moreover, low levels of oxygen in tumor tissue may signal that the first or second-line therapy will not be successful. This knowledge triggers the inevitable search for different kinds of treatment that will successfully cure aggressive tumors. Due to its exclusive expression on cancer cells, carbonic anhydrase IX belongs to the group of the most precise targets in hypoxic tumors. CA IX possesses several exceptional qualities that predetermine its crucial role in targeted therapy. Its expression on the cell membrane makes it an easily accessible target, while its absence in healthy corresponding tissues makes the treatment practically harmless. The presence of CA IX in solid tumors causes an acidic environment that may lead to the failure of standard therapy.

Methods

Parental mouse hybridomas (IV/18 and VII/20) were humanized to antibodies which were subsequently named CA9hu-1 and CA9hu-2. From each hybridoma we obtained 25 clones. Each clone was tested for ADCC and CDC activity, affinity, extracellular pH measurement, multicellular aggregation analysis and real-time monitoring of invasion with xCELLigence system.

Results

Both CA9hu-1 and CA9hu-2 are IgG1 antibodies and they were both examined *in vivo.* Here we describe anti-CAIX antibodies that can reverse the failure of standard therapy as a result of an acidic environment by modulating the TME. CA9hu-1 is directed at the conformational epitope of the catalytic domain, while CA9hu-2 targets the sequential epitope of the proteo-glycan domain. They are both able to induce an immune response, have high affinity, as well as ADCC and CDC activity. While the first one internalizes after binding to the antigen, the second one is able to reduce metastases formation. More importantly, they have both proved the ability to block the acidification of the extracellular environment.

Conclusion

CA9hu-1 and CA9hu-2 are the very first humanized antibodies against CA IX that are likely to become suitable therapies for hypoxic tumors. These antibodies can be applied in the treatment therapy of primary tumors and suppression of metastases formation.

Introduction

Hypoxia is an intrinsic property of solid tumors defined as a condition where partial O_2 pressure is below 10 mmHg [1, 2]. Hypoxic tumor microenvironment (TME), caused by angiogenic dysregulation and consequent disruption of the vascular network, leads to metabolic and genomic changes [3]. At the molecular level, adaptation of tumor cells to the hypoxic TME is largely mediated by the hypoxia

inducible factor (HIF) family of transcription factors [4]. HIF targets include genes encoding mediators of angiogenesis such as vascular endothelial growth factor (VEGF) and VEGF receptors, enzymes of the glycolytic pathway such as hexokinase 2, lactate dehydrogenase, and glucose transporters (GLUT-1, GLUT-3), as well as pH regulators including carbonic anhydrase IX (CA IX) [5–7].

CA IX is one of the best responders to low oxygenation because of its transcriptional regulation, driven mainly by HIF-1 that binds to a hypoxia-response element (HRE) consensus sequence localized near the transcription initiation site of the *CA9* gene [8]. CA IX is a highly active member of the family of carbonic anhydrases which differs from the other CA isoforms by strong association with cancer, hypoxia-related expression pattern, acidic pKa optimum and a unique proteoglycan-like domain (PG) protruding from the globular catalytic domain of the enzyme [9–13]. CA IX is functionally involved in diverse aspects of cancer development, including protection of cancer cell survival in conditions of hypoxia and acidosis, facilitation of cancer cell migration and invasion, contribution to metastatic dissemination, homing and growth of metastatic lesions [14–19].

Hypoxia is a hallmark of solid tumors that has been linked to increased tumor metastasis and poor prognosis in cancer patients [1, 2]. Hypoxic tumor microenvironment does not only enhance proliferation and invasiveness of tumor cells, but also allows them to evade the immune system, impair drug delivery, further increasing immunotherapy and chemotherapy resistance, conferring them a survival advantage [20]. The presence of hypoxic areas is closely correlated with tumor progression and propagation of more aggressive and stress-resistant subpopulations where CA IX plays a critical adaptive role. Therefore, targeting hypoxia-induced molecules such as CA IX has a high potential for therapeutic benefits [21–23]. Numerous published studies on the role of CA IX in tumor biology and its clinical value support the view that it can serve as a biomarker and/or a therapy target in diverse tumor types and settings [24, 25]. These studies provide arguments in favour of using CA IX for cancer immunotherapy. First, CA IX is associated with hypoxia, acidosis and aggressive tumor phenotype and thus expressed in a situation when available immunotherapy often fails. Second, CA IX is a very stable protein localized on the cell surface, and therefore it is accessible to antibodies binding to its extracellular domains.

In the past, a collection of eleven anti-CA IX murine monoclonal antibodies was generated and characterized by Zatovicova [26]. However, the clinical use of murine monoclonal antibodies in cancer patients is highly limited due to human anti-mouse antibody response (HAMA). Thus, we selected the two most promising antibodies for humanization in order to explore their full therapeutic potential.

Here we describe the construction and characterization of anti-CA IX antibodies named CA9hu-1 and CA9hu-2, which are the humanized versions of the murine monoclonal antibodies VII/20 and IV/18, specifically binding to distinct extracellular domains of CA IX and exhibiting disparate capabilities to induce CA IX internalization. We show that the humanization process completely preserved the binding specificity and affinity of the original mouse antibody. In addition, CA9hu-1 and CA9hu-2 acquired desirable effector functions, especially the capability for strong ADCC, antibody-dependent cell-mediated phagocytosis (ADPC) and complement dependent cytotoxicity (CDC) in *in vitro* assays with human

cancer cells and human effector cells. We also demonstrate the ability of the new antibodies to block the function of CA IX in pH regulation and invasiveness of tumor cells. Clinical grade humanized antibodies CA9hu-1 and CA9hu-2 are now being produced for the first-in-human clinical trials.

Materials And Methods

Construction and characterization of humanized antibody variants CA9hu-1 and CA9hu-2

Humanization of VII/20 and IV/18 murine antibodies was performed by Fusion antibodies (Belfast, N. Ireland). After the RNA isolation from the pellets of hybridoma cells, cDNA was created by reverse-transcription with an oligo(dT) primer. PCR reactions were set up using variable domain primers to amplify both the V_H and V_L regions of the monoclonal antibody DNA. The V_H and V_L cDNAs were cloned and analysed by DNA sequencing. After the VII/20 and IV/18 murine antibodies variable domains were sequenced, the CDRs were identified using antibody-numbering systems from IMGT and Kabat [27, 28]. For optimal retention of CDR-loop conformation, both numbering systems were used to identify a combined IMGT/Kabat CDR sequence of the murine antibody. Sequence analysis of the murine antibody was followed by humanized variant alignment. CDRs of the murine V_H and V_L were grafted into the acceptor frameworks. The combination of five VH and five VL chains resulted in generation of twenty-five humanized variants having humanized variable domains [marked in the following text as heavy (HC) and light (LC) chain] and human Ig constant domains.

Cell culture and transfection

Human cells with endogenous, hypoxia-inducible expression of CA IX: BT-20 (ATCC HTB-19) derived from breast carcinoma; JIMT-1 human breast carcinoma cells (HMS LINCS Database ID: 51118); MDA-MB-231 breast carcinoma cells (ATCC HTB-26); MBA-MB-468 (ATCC HTB-132); HT1080-iRFP670 cells (human fibrosarcoma cell line); 8-MG-BA human glioblastoma cancer cells (Cellosaurus CVCL_1052) and 42-MG-BA human glioblastoma cancer cells (Cellosaurus CVCL_1798) were cultivated under standard conditions in Dulbecco's modified Eagle's medium (BioSera, Nuaille, France) supplemented with 10% fetal calf serum (BioWhittaker, Basel, Switzerland) and gentamicine (Sandoz, Holzkirchen, Germany) in humidified air containing 21% O_2, 5% CO_2 at 37°C and in hypoxic conditions at an anaerobic workstation (Ruskinn Technologies, Bridgend, UK) in a humidified atmosphere containing 1% O_2, 5% CO_2, 10% H_2 and 84% N_2 at 37°C. Experiments described in this paper were performed with C-33a human cervical carcinoma cells (ATCC HTB-31) and B16 F0 (ATCC CRL-6322) mouse melanoma cells transfected with the full-length human *CA9* cDNA (C-33a_CA IX; B16-CA IX) in pcDNA3.1 + plasmid [29]. Related mock-transfected cells served as negative controls. Transfections were performed using TurboFectTM transfection reagent (Thermo Fisher Scientific, MA, USA). To obtain stable polyclonal cell lines, transfected cells were subjected to selection in G418 for 2 weeks and then separated on magnetic beads (Dynabeads M-450 Tosylactivated, Invitrogen, CA, USA) coupled to the CA IX-specific M75 monoclonal antibody according to

manufacturer´s instructions. Separated cell subpopulations were expanded and CA IX expression was analysed by flow cytometry, western blotting and immunofluorescence.

ELISA screening of humanized antibodies

Preparation of antigens for ELISA: Protein extract from human cervical cancer cells C-33a permanently transfected with the full-length CA9 cDNA (C-33a_CA IX) was used as a screening antigen. Lysate from mock-transfected cells was used as a negative antigen control (C-33a_neo). Proteins were extracted from the cell monolayer with RIPA lysis buffer (0.1% deoxycholate, 1% Triton X-100 and protease inhibitor cocktail in PBS). Protein concentrations were determined by bicinchoninic acid assay (ThermoFisher Scientific, Waltham, MA USA) according to the manufacturer's instructions and diluted to final concentration 0.2 mg/ml in PBS.

ELISA procedure: 50 µl of either CA IX-positive or CA IX-negative protein extract was coated on the surface of high binding microplate wells (Greiner bio-one) overnight at 37°C. After washing with PBS-T (0.05% Tween-20 in PBS pH 7.2), 50 µl of all humanized variants (diluted to concentration 5 µg/ml in 10% FCS in PBS-T) were added and incubated for 2 h at room temperature. Peroxidase-labelled swine anti-human IgG (diluted 1:5,000 in 10% FCS in PBS-T; Sigma-Aldrich, St. Louis, MO USA) was used as a detector. Parental IV/18 and VII/20 antibody (marked as "mouse Ab") as well as chimeric HC0LC0 antibody (having the murine variable domains and the human Ig constant domains) were used as reference samples. Results are expressed by O.D. values of absorbance measured at 492 nm.

Differential ELISA

For the CA IX domain differential ELISA, the wells were coated with the following antigens: RIPA extract of C-33a cells permanently transfected with the full-length CA9 cDNA (C-33a_CA IX), del PG CA9 cDNA (ΔPG) and del catalytic domain CA9 cDNA (ΔCA) in pcDNA3.1 + plasmid diluted to final concentration 0.2 mg/ml in PBS and were then assayed as above.

SPR procedure setup

SPR (Surface plasmon resonance) analysis of antibody-antigen interactions was performed using Biacore technology (R&D grade) by Biaffin GmbH & Co KG, in Kassel, Germany. Each humanized antibody variant was captured on the sensor chip and recombinant human CA IX protein (rh CA IX; 42 kDa; R&D systems) was added to the buffer flowing over the chip. Affinity measurements were performed using Biacore T200 instrument and settings details of quantitative interaction analysis between antibodies and rh CA IX protein were as follows: Flow rate: 30 µL/min for kinetic interaction analyses. Analysis temperature: 25°C. Analysis buffer: 10 mM HEPES pH 7.4, 150 mM NaCl, 3 mM EDTA, 0.05% Tween 20. Sensor chips CM5. Setup: Preparation of an α-human Fc capture surface, reversible capturing of antibodies, interaction analyses with antigen 1.56–400 nM rh CA IX (42 kDa), and complete removal of antibody-antigen complex.

Immunofluorescence assay

C-33a_CA IX cells (300,000 cells per Petri dish) were plated on glass coverslips 24 h before the experiment and cultivated in different conditions: pH 7.2; pH 6.6, normoxia and hypoxia. Cells grown on glass coverslips were incubated with antibody (5 µg/ml) for 1 h at 37°C, gently washed with PBS, and fixed in ice-cold methanol at − 20°C for 5 min. Nonspecific binding was blocked by incubation with PBS containing 1% BSA for 30 min at 37°C. Cells were then visualized by an antihuman Alexa Fluor® 488-conjugated antibody (Invitrogen, CA, USA) diluted 1:1,000 in the blocking buffer for 1 h at 37°C. The nuclei were stained with DAPI (Sigma-Aldrich, MO, USA). Finally, the coverslips were mounted onto slides in the Fluorescent Mounting Media (Sigma-Aldrich, MO, USA), and analysed by the confocal laser scanning microscope Zeiss LSM 510 Meta.

Immunofluorescence internalization assay

C-33a_CA IX, JIMT-1, BT-20, MDA-MB-468, MDA-MB-231 and C-33a_neo cells (300,000 cells per Petri dish) were plated on glass coverslips 24 h before the experiment. The live cells were incubated with the antibody (50 µg/ml) diluted in culture medium at 4°C for 30 min to recruit the mAb to CA IX on the cell surface. Subsequently, the cells were washed to remove any unbound antibody, and transferred to 37°C for 3 h to induce internalization, or fixed in ice-cold methanol at − 20°C for 5 min. At the end of the 3 h treatment period, the cells were washed and fixed. After blocking the primary antibody was visualised using anti-human Alexa Fluor® 488 secondary antibodies (Invitrogen, CA, USA, 1:1,000 in 1% BSA). Finally, the cells were mounted onto slides and analysed by the confocal laser scanning microscope Zeiss LSM 510 Meta.

ADCC

ADCC reporter assay was performed according to the manufacturer's instructions using C-33a_CA IX, C-33a_neo cells as well as cancer cells expressing CA IX induced by hypoxia (breast cancer BT-20 and JIMT-1 and glioblastoma 8-MG-BA and 42-MG-BA). Cells (12,500 cells/well) were plated onto sterile 96-well plates and incubated in culture medium overnight at 37°C. Humanized antibody variants (CA9hu-1 or CA9hu-2) were diluted to 1 µg/ml in PBS and 75,000 of effector cells (according to the recommended effector: target ratio 6:1) were used per well. After 6 hours of incubation, detection of firefly luciferase was performed using Bio-GloTM Luciferase Assay Reagent (Promega). Mixture of samples with ADCC assay buffer and effector cells without adding the humanized antibody is marked as "no Ab". Mixture of samples without antibody and effector cells is marked as "no Ab, no EC", and serves as "plate background". Results are expressed as luminescence in relative luminescence units (RLU). For EC_{50} determinations target cells were incubated with a series of concentrations of antibodies, followed by addition of ADCC Bioassay Effector Cells. The E:T ratio was 6:1. After 6 hours of induction at 37°C, Bio-Glo™ Luciferase Assay Reagent was added and luminescence was determined using a GloMax®-Multi + Luminometer. Data were fitted to a 4PL curve using GraphPad Prism® software.

ADPC

To evaluate the ability of humanized antibodies to mediate phagocytosis, ADCP Reporter Bioassay System (Promega) was applied. ADCP reporter assay was performed according to the manufacturer's instructions using C-33a_CA IX as well as C-33a_neo cells. One day before analysis, 12,500 cells per well were plated onto a sterile 96-well plate and incubated in culture medium overnight at 37°C. Humanized antibody variants CA9hu-1(HC4LC4) and CA9hu-2(HC4LC5) were diluted to 2 µg/ml in PBS and 75,000 of effector cells (according to the recommended effector:target ratio of 6:1) were used per well. After 6 hours of incubation, detection of firefly luciferase was performed using Bio-Glo™ Luciferase Assay Reagent (Promega).

CDC

Twenty-four hours before the assay, C-33a_CA IX as well as C-33a_neo cells were plated onto a sterile 96-well plate in concentration of 20 x 10^4 cells per well in 50 µl of DMEM culture medium with 10% FCS and incubated overnight in CO_2 incubator with 5% CO_2 at 37°C. On the day of the analysis, CDC assay was performed using rabbit complement serum (BAG Healthcare). First, culture medium was removed from each of the wells and 50 µl of the fresh culture medium with 10% FCS and 50 µl antibody diluted to 5 µg/ml was added per well. Samples without antibody were used as "no antibody" control. The mixture was incubated at room temperature for 5 min and 10 µl of rabbit complement serum was added to each well, mixed and cultured at standard condition for 24 h. After incubation, cell viability was analysed by CellTiter-Blue® Cell Viability Assay, Promega) according to the manufacturer´s instructions. The fluorescence was recorded with 530nm/590nm (excitation/emission) filter set using Bio-Tek Synergy HT microplate reader.

Measurement of extracellular pH

Before the assay, C33a_CA IX cells were seeded onto 24-well plate HydroDish® (105,000 cells/well) and allowed to attach for 3–5 h. Subsequently, culture medium was replaced with medium containing lowered bicarbonate and serum (1 ml/well) to mimic conditions characteristic for tumours. We used DMEM medium (Sigma-Aldrich) supplemented with 4.5 g/l glucose, 22 mM $NaHCO_3$, 1% FCS, 4 mM glutamine and 1mM pyruvate with the presence or absence of humanized antibodies CA9hu-1(HC4LC4) or CA9hu-2(HC4LC5) and control irrelevant IgG (50 µg/ml). Cells were incubated in hypoxia (1% O_2, 5% CO_2, 10% H_2 and 84% N_2, Ruskinn Technology, at 37°C) for next 72 h and pH of culture medium was analysed by non-invasive online pH monitoring using pH measuring device SDR SensorDish® Reader (PreSens Precision Sensing GmbH).

Multicellular aggregation analysis

The non-ionic acid poly(2-hydroxyethyl methacrylate) (poly-HEMA; Sigma-Aldrich), which inhibits matrix deposition and cell attachment, was dissolved in 99% ethanol at 10 mg/ml. 6-well tissue culture plates were coated with 0.5 ml of poly-HEMA solution, allowed to dry, washed with PBS and stored at 4°C. C-33a_CA IX cells (400,000 cells/well) were added to poly-HEMA-coated wells and cultured in the presence or absence of humanized antibody variant (30 µg/ml) for 24 and 72 h. To evaluate the ability of C-33a_CA IX cells to form multicellular aggregates, images from either treated or untreated cells were

acquired and the accumulated pixel density was measured using the ImageJ software. At the end of the longer treatment (72 h), C-33a_CA IX cells were recovered, centrifuged, and subsequently analysed via flow cytometry using propidium iodide to stain dead cells.

Real-time monitoring of invasion with xCELLigence system

The xCELLigence cell index impedance measurements were performed using the CIM-Plate16 placed in the RTCA DP station according to the instructions of the supplier (Roche, Basel, Switzerland). Cells were trypsinised, resuspended at the density of 400,000 cell/ml in serum-free medium, added to the Matrigel coating top chamber of the CIM-Plate and allowed to invade towards bottom chamber containing medium with 10% FCS as a chemoattractant. The CIM-Plate 16 was placed in the RTCA DP station and migration was monitored every 15 min for 100 h in hypoxic conditions (1% O_2).

In vivo experiments

NMRI-Foxn1^{nu} nu/nu female mice and C57BL/6J female mice (Charles River Laboratories, Inc.) were housed in SPF facility and used in accordance with the Institutional Ethic Committee guidelines under the approved protocols. The project was approved by the national competence authority – State Veterinary and Food Administration of the Slovak Republic (No. Ro. 4245/13–221 and 292/16-221g) in compliance with the Directive 2010/63/EU and the Regulation 377/2012 on the protection of animals used for scientific purposes. Mice were housed in groups of 3 randomised animals in individually ventilated IVC (Tecniplast) cages with wooden fibre bedding, at 20 +/- 2°C temperature, using natural light/dark cycle, with SNIFF diet, ad libitum access to food and water, with environmental enrichment by paper houses. The mice were subjected to regular monitoring with humane endpoint. The number of mice were kept at minimum required to achieve statistical significance; *in vivo* study was designed based on thorough preceding *in vitro* experiments. Primary tumors were generated by a subcutaneous injection of a suspension of B16-FL-CA IX melanoma cells (5x10^5 cells in 100 µl PBS) into the right and left upper flank of NMRI-Foxn1nu nu/nu male mice (n = 3). During the experiment, the antibodies were intravenously administered (100 µg in 100 µL PBS) on the 0, 5th, 8th, 12th and 15th day. Mice were sacrificed on the 16th day after inoculation. For the lung colonization assay, hypoxia pre-incubated HT1080-iRFP670 cells were treated or non-treated with IV/18 to block PG-domain of CA IX protein. Cells were injected into the tail vein (1.5 × 10^6/mouse) of NMRI nude mice (NMRI-Foxn1^{nu} nu/nu female mice, Charles River Laboratories, Inc., 10 mice/group). During the experiment, the antibodies were intravenously administered (50 µg in 100 µL PBS) every three days. After 12 days mice were sacrificed. PBS-perfused lungs were *ex vivo* evaluated for fluorescent signal emitted by metastasizing cancer cells using an IVIS system (*In vivo* Imaging System, Caliper Life Sciences).

Statistical analysis

Continuous variables were expressed as mean ± SEM and evaluated either by ANOVA or by Student t-test (between two groups). A $p < 0.05$ was considered significant (*).

Results

Anti-tumor effects of parental murine monoclonal antibodies

Excellent properties and characteristics of previously described anti-CA IX mouse monoclonal antibodies VII/20 targeting catalytic CA-domain and IV/18 specific to PG-domain [26] predetermined them as the basis for generation of humanized antibodies for anti-cancer therapeutic application. Biological properties of the VII/20 mAb and its capacity to reduce tumor growth were evaluated earlier in mouse xenograft model of HT29 colorectal carcinoma [30].

Here we investigated the anti-cancer effect of both IV/18 and VII/20 antibodies on the growth of primary tumors in subcutaneous xenografts formed from mouse melanoma cells. $5x10^5$ mouse melanoma B16-F0 cells stably transfected with human CA IX and 50 µg of antibody were injected subcutaneously into the left and right flank region of mice. During the experiment, the antibodies were intravenously administered every three days. Results showed that both antibodies significantly reduced tumor weight when compared to the control, non-treated animal (marked as “Ctrl”), (Fig. 1A, B).

We further evaluated the ability of the antibodies to attenuate cancer cell extravasation and metastasis formation in a murine lung colonization model. Metastatic colonies of fluorescently tagged HT1080-RFP cells in murine lungs were imaged *ex vivo* 12 days after injection using IVIS Caliper imaging system, in which total radiant efficiency reflects the amount of cancer cells in murine lungs. Pre-incubation of HT1080-RFP cells with mAb IV/18, and subsequent administration of 3 doses of antibodies (50 µg/mouse) during 12 days after the initial tail vein injection ($1.5x10^6$ cells per animal, 10 mice per group) caused a marked decrease in lung colonisation by these cells (Fig. 1C). Since the metastatic colonies were evaluated *ex vivo* relatively shortly after the tail vein inoculation (12 days), reduced extravasation was apparently the main factor behind the decreased metastasis formation following treatment with IV/18 antibody (Fig. 1D).

Humanization of VII/20 and IV/18 antibodies

Based on *in vivo* anti-tumor properties of CA IX-specific VII/20 and IV/18 murine monoclonal antibodies, we decided to generate their humanized versions for human anti-cancer therapy. Humanization of anti-CA IX antibodies was achieved by complementarity-determining region (CDR) grafting approach. A number of human framework sequences (coming from mature human IgG from a human source) were identified and used as "acceptor" frameworks for CDR sequences. Thus, the humanized sequences are expected to be non-immunogenic and retain the canonical structure of the CDR-loops. DNAs coding for the amino acid sequence of humanized variants were synthesized and cloned into an appropriate mammalian expression plasmid. 25 humanized variants of CA9hu-1 from the parental mouse antibody VII/20 and 25 variants of CA9hu-2 from the mouse antibody IV/18 were created comprising murine-derived CDRs and humanized heavy and light regions.

CA IX-binding properties of the humanized CA9hu-1 and CA9hu-2 antibodies

An ideal antibody humanization should be capable of maintaining the specificity and affinity towards the antigen comparable with parental mouse immunoglobulin. However, the loss of specificity and affinity of antibody to its specific target is the main problem of humanization [31]. For this reason, all antibody variants of CA9hu-1 and CA9hu-2 were screened for specific binding and affinity towards the human CA IX antigen by ELISA using antigens prepared from stably transfected C-33a cell line expressing CA IX (C-33a_CA IX) and parental mock-transfected C-33a cells without CA IX expression (C-33a_neo). The results show that both humanized antibodies retained specific and effective binding similar to or exceeding that of the parental antibodies (Supplementary Fig. 1). In case of CA9hu-1 (Supplementary Fig. 1A), HC4 variants exhibited the highest binding efficiency against CA IX. Similarly, the highest binding efficiency was observed in case of HC3 and HC4 variants of CA9hu-2 antibody (Supplementary Fig. 1B).

To evaluate the CA IX domain-specificity of the humanized antibodies, the representative antibody variants CA9hu-1 (HC4LC4) and CA9hu-2(HC4LC5) were analysed by ELISA against the CA IX protein with deletions in PG and catalytic domains, respectively. In line with the specificity of the parental antibodies, CA9hu-1 (HC4LC4) binds to catalytic domain, while CA9hu-2 (HC4LC5) is directed against the PG domain (Supplementary Fig. 1C).

Antigen-binding affinity of all humanized variants was assessed by SPR using a Biacore instrument. Results of real-time monitoring of their binding kinetics with recombinant human CA IX protein are expressed as the equilibrium dissociation constant (K_D). As shown in Table 1 (Supplementary data), all antibody variants possess K_D values in a low nanomolar range ($10^{-7} – 10^{-9}$) that is generally considered to be the range of high affinity antibodies. Moreover, some antibody variants of CA9hu-1 (HC4LC1, HC4LC2, HC4LC3, HC4LC4 and HC4LC5) showed even higher affinity than the chimeric variant.

Membrane CA IX binding and internalization of the humanized antibodies

There are several arguments in favour of CA IX being a suitable target molecule for cancer therapy. One of the strong reasons is the CA IX exposure on the cell surface and its accessibility to an antibody from the extracellular space. Indirect immunofluorescence demonstrated that both of the antibody variants CA9hu-1 (HC4LC4) and CA9hu-2 (HC4LC5) bound specifically to the CA IX antigen localized at the surface of transfected cells C33a_CA IX at 37°C in sparse cell culture as well as in high cell density and also in acidic and hypoxic conditions (Fig. 2).

Effective applications of monoclonal antibodies in cancer therapy rely on their ability to specifically target cancer tissues but, in some cases, also to enter the intracellular space via receptor-mediated internalization. Since CA9hu-1 antibody was derived from the internalizing murine antibody VII/20 [30], we wanted to find out, whether this capability was preserved during the humanization process. Using C33a_CA IX cells that express high levels of CA IX and employing also collection of carcinoma cells with natural CA IX expression, we demonstrated that CA9hu-1 (HC4LC4) antibody directed to the catalytic domain of CA IX is able to induce the CA IX-mediated internalization (Fig. 3). The cells were allowed to bind mAbs at 4°C for 30 min and incubated for 3 h at 37°C to enable internalization. After washing of

unbound antibodies, cells were fixed with methanol and treated with Alexa Fluor® 488-conjugated secondary antibody to visualize the primary mAbs. CA9hu-1 (HC4LC4) antibody was accumulated in the cytoplasm after incubation at 37°C showing its internalization. We examined the internalization of CA9hu-2 under the same conditions. The fluorescence signal in the cytoplasm was extremely low (data not shown), it was almost undetectable.

Cytotoxicity-inducing effector functions of humanized CA IX-specific antibodies

The main expected role of the new anti-CA IX humanized antibodies in cancer immunotherapy is to stimulate the host immune system to attack the CA IX expressing cancer cells. The underlying mechanisms include natural killer (NK) cell-mediated antibody-dependent cellular cytotoxicity (ADCC), macrophage-mediated antibody-dependent cell phagocytosis (ADCP), and/or complement-dependent cytotoxicity (CDC). We therefore examined the capacity of our humanized antibodies to induce these effector functions.

Ability of humanized antibody variants to mediate the antibody-dependent cytotoxic effect was evaluated using ADCC reporter bioluminescence assay [32]. The assay employs engineered Jurkat cells stably expressing the FcγRIIIa receptor, V158 high affinity variant, and NFAT (nuclear factor of activated T-cells) response element driving expression of firefly luciferase, as effector cells. The ADCC response was quantified through the luciferase production as a result of NFAT activation. As shown in Fig. 4A, B, CA9hu-1 and CA9hu-2 variants exhibited high luminescence signal and thus, high cytotoxicity against C-33a_CA IX expressing cells. As the RLU of samples were 100 times higher than the plate background RLU (marked as "no Ab, no EC cells"), there was no need to subtract plate background from the sample RLU. Although CA9hu-2 variants appeared to be less efficacious than CA9hu-1 antibodies, they still possess two times higher capacity to activate the cytotoxic pathway via ADCC against C-33a_CA IX expressing cells than against C-33a_neo cells.

To prove the antibody-dependent cell-mediated cytotoxicity on cancer cells naturally expressing CA IX, we analysed TNBC cell lines BT-20 and JIMT-1 as well as glioblastoma cell line 42-MG-BA. Figure 4C, D clearly shows that selected humanized antibody variants CA9hu-1 (HC4LC4) and CA9hu-2 (HC4LC5) can activate the ADCC pathway and mediate cytotoxic effect on target cells expressing CA IX. The highest induction (> 25-fold) was observed in TNBC cells BT-20 after the treatment with CA9hu-1 (HC4LC4) antibody. In addition, we calculated the EC_{50} for both humanized variants. The EC_{50} value of CA9hu-1 variant response using C33a_CA IX, BT-20 or JIMT-1 target cells was 51 ng/ml, 72 ng/ml and 107 ng/ml respectively, which is comparable to EC_{50} of therapeutic antibodies trastuzumab and cetuximab (as declared by the ADCC assay manufacturer).

The ability of humanized antibody variants to participate in complement-dependent cytotoxicity (CDC), was determined by incubation of rabbit serum with CA IX-positive C-33a_CA IX cells, and C-33a_neo cells in presence of tested antibody and recorded using cell viability assay after 24 h. Measured fluorescence data are shown in Fig. 5A. Complement binding and activation analysis showed that CA9hu-1 (HC4LC4)

and also CA9hu-2 (HC4LC5) antibody variants can induce cytostatic response of CA IX-positive C-33a_CA IX cells in presence of complement when compared to no-antibody control. This was not observed in CA IX-negative cell line C-33a_neo. The results demonstrate that humanized variants of both CA9hu-1 and CA9hu-2 can be used to specifically distinguish and consequently mediate cytotoxic effect on tumor cells expressing CA IX via CDC.

For *in vitro* analyses of the ability of humanized antibody variants CA9hu-1 (HC4LC4) and CA9hu-2 (HC4LC5) to mediate phagocytosis, we used an ADCP reporter bioluminescent cell-based assay, which measures the potency and stability of antibodies and other biologicals containing Fc domains that specifically bind and activate FcγRIIa. The assay uses engineered Jurkat T cells expressing the FcγRIIa receptor, H131 high affinity variant, and NFAT response element driving expression of firefly luciferase as effector cells. Thus, ADCP mechanism of action is quantified through the luciferase production as a result of NFAT activation. Results are expressed as luminescence in relative luminescence units (RLU).

As shown in Fig. 5B, almost no phagocytic activity was observed when CA IX-negative C-33a_neo cells were used as target cells independently of presence or absence of CA IX-specific antibodies. The phagocytic potency was acquired after the incubation of CA IX-expressing cancer cells in the presence of humanized antibody variant CA9hu-1 (HC4LC4) (236%) and also CA9hu-2 (HC4LC5) (185%). These results demonstrate that both humanized antibody variants can be used to specifically recognize and consequently mediate phagocytosis of cancer cells expressing CA IX. Considering the fact that ADCP is an important mechanism of action of therapeutic antibodies, the phagocytic potency of the humanized antibody represents an extraordinary and beneficial property.

Effects of CA9hu-1 and CA9hu-2 antibodies on biological functions of CA IX

Therapeutic approaches targeting CA IX have primarily focused on the development of specific monoclonal antibodies which are able to detect and kill tumor cells expressing CA IX in cooperation with the immune system. The second approach for targeting CA IX-cancer cells involves the utilization of antibodies for blocking the functions of CA IX in tumor biology, especially its pro-survival role in protecting tumor cells in hostile acidic microenvironments and in adhesion–migration–invasion.

First, we evaluated the effects of humanized antibodies on multicellular aggregation of cancer cells during extracellular matrix (ECM)-detachment, which represents an efficient mechanism for anoikis inhibition. As it is known detachment of the cells from the extracellular matrix initiates programmed cell death by a process termed anoikis. Malignant cells must acquire anoikis resistance to leave the primary tumour and metastasise. Resistance to anoikis plays a major role in tumor metastasis as tumor cells that survive after detachment from their primary location can travel through circulatory systems. Emerging evidence suggests that as tumor cells lose the requirement for anchorage dependency for growth and survival, they increasingly rely on their ability to adhere to each other (that is, multicellular aggregation) for survival. Figure 6A shows that the humanized antibodies CA9hu-1 (HC4LC4) and CA9hu-2 (HC4LC5) reduce the ability of C-33a_CA IX cells to form multicellular aggregates during detached condition on poly-HEMA coated dishes. To validate the enhanced sensitivity of C-33a_CA IX cancer cells treated with

the humanized antibody, we performed flow cytometry and propidium iodide staining. Figure 6B shows that antibodies affect the viability of treated cells after 72 h growth in detached conditions. The percentage of dead cells treated with CA9hu-1 (HC4LC4) and CA9hu-2 (HC4LC5) was 37.3% and 35.1% respectively. In case of C-33a_CA IX cells without antibody treatment ("negative control"), we observed only 15.7% ± of dead cells. The data demonstrates the ability of humanized antibody variants to reduce multicellular aggregation of C-33a_CA IX-expressing cancer cells and subsequently to enhance their sensitivity to anoikis.

To validate the ability of humanized antibody variants to affect extracellular acidosis by targeting and blocking CA IX, pH of cell culture media was measured by a non-invasive online pH monitoring using pH measuring device SDR SensorDish Reader. C-33a_CA IX cells were grown in monolayer and incubated in hypoxia (1% O_2) in the presence of humanized antibodies CA9hu-1 (HC4LC4) or CA9hu-2 (HC4LC5) or control irrelevant IgG1 (50 µg/ml) for 72 h. The results show that treatment with humanized antibody variants led to reduced extracellular acidosis in hypoxic cells Fig. 7A.

To investigate the effect of humanized antibodies on cancer cell invasion, we performed the *in vitro* xCELLigence cell index impedance measurements using CIM-Plate16 and RTCA DP station. C-33a_CA IX cells were resuspended in serum-free medium in the presence or absence of humanized antibody variant CA9hu-1 (HC4LC4) and CA9hu-2 (HC4LC5). After addition to the matrigel-coated top chamber of the CIM-Plate, C-33a_CA IX cells were allowed to migrate towards bottom chamber containing medium with 10% FCS as a chemoattractant. The foregoing results in Fig. 7B and C demonstrate the ability of the humanized antibody variants to inhibit invasion of CA IX-expressing C-33a cells. Considering the fact that inhibition of cancer cell invasion could lead to limited tumor progression, and consequently, to reduced mortality of cancer patients, this mechanism of action represents an extraordinary beneficial property. Additionally, this is the first demonstration of an aforementioned effect described using PG domain-specific humanized antibodies.

Discussion

Biological treatment with human or humanized antibodies is one of the most effective and clinically significant therapies that are currently available on the market. Every year regulators such as EMA or FDA approve increasing numbers of drugs with an antibody basis, and there are already many of them proven and used in clinical practice. In the past decade there have been approximately fifty new antibodies approved, with the total of more than sixty monoclonal antibodies (mAbs) used in the clinic [33]. Yet most of the mAbs, either tested in clinical trials or already authorised for the treatment, target the same antigens, and the number of newly developed antibodies directing at novel targets is not so high [34].

Considering the high number of oncogenes and tumor-associated proteins, we can expect development of many new therapeutics for oncological diseases. This expectation emerges from the significantly lower risk of side effects posed by therapies based on humanized antibodies in comparison with conventional therapeutics, although adverse events can occur [35]. Negative outcomes of clinical

development are often related to the ineffectiveness of the immunotherapy rather than a threat to patient's health, and the failure is often associated with poor patient stratification.

Almost 600 mAbs have been examined in clinical trials around the globe since the 1990s, out of which about 30 mAbs are now available for the cancer therapy. This remarkable progress in cancer treatment has greatly affected the percentage of treatable diseases in practically all types of tumors. The cancer research is now facing another challenge – how to approach the remaining cases where available therapy is still failing? How to treat, for example, TNBC patients that become resistant to HER2-directed treatment?

The most aggressive tumors are often hypoxic. Targeted therapy against these hypoxic tumors must therefore be the highest priority in the near future. The common feature of hypoxic tumors is their resistance to chemotherapy and radiotherapy. Furthermore, hypoxic tumors often do not respond to immunotherapy due to several factors such as acidic TME, increased invasiveness, metastases, inadequate immune response, genomic instability, metabolic reprogramming, or vascularization. The gap in the treatment of hypoxic tumors may lie in the lack of antibodies targeting HIF-1-dependent genes that are upregulated in response to hypoxia and mediate pro-survival pathways.

Carbonic anhydrase IX belongs to a broad group of HIF-1 targets. It is currently one of the best markers of poor prognosis related to hypoxia. Low O_2 levels do not only regulate CA IX expression on the transcription level, but also affect its enzymatic activity and splicing (important for the correct localization and catalytic activity). Another compelling advantage of CA IX is its easy accessibility given the localization on the plasma membrane. CA IX is key to pH regulation in tumors that increases the acidity of tumour microenvironment and plays an important role in the invasiveness of tumor cells. Furthermore, CA IX expression is strongly associated with tumor phenotype. All these attributes make CA IX an attractive therapeutic target.

To date, several mAbs against human CA IX have been extensively studied. Most of the studies including the clinical trials were performed in clear cell renal cell carcinomas (ccRCC) models and patients using the chimeric monoclonal antibody G250 known under commercial names RENCAREX® or GIRENTUXIMAB®. In most ccRCC tumors, CA IX is frequently expressed at high levels due to the functional inactivation of VHL tumor suppressor gene that generates defective pVHL protein unable to negatively regulate HIF-1α [36]. Monoclonal antibody G250 and its humanized, chimeric and bispecific variants were systematically studied in pre-clinical ccRCC models and in clinical cohorts of ccRCC patients [37–40]. This antibody showed good safety, tolerability and promising efficacy profile in Phase I and II clinical trials with more than 100 patients with metastatic RCC [41, 42]. Phase III clinical trial (ARISER), targeted at patients with non-metastatic renal cell carcinoma showed no significant improvement of disease-free survival among randomized/non-stratified patients treated with RENCAREX® compared to placebo. However, more careful, but retrospective analysis of the data showed that patients with a high tumor CA IX scores have prolonged disease-free survival of about 22 months [43].

In addition, several human CA IX-specific monoclonal antibodies directed to catalytic domain have been described, but their characterization did not go beyond the preclinical phase [44, 45]. On the other hand, catalytic domain-specific human BAY79-4620 antibody showed potent antitumor efficacy in xenograft models, but failed in an early clinical trial due to inadequate toxicity caused by toxin conjugated via self-cleavable linker [46]. Thus, except GIRENTUXIMAB®, that would require re-evaluation in improved trial settings, there is currently no CA IX-directed therapeutic antibody under clinical development.

Thus, CA9hu-1 and CA9hu-2 humanized antibodies appear to be promising candidates to fulfil this unmet need. The CA9hu-1 humanized antibody recognizes the exofacial catalytic domain of the CA IX protein. It has several unique characteristics that predetermine its strong anti-cancer effect: high affinity and specificity, absence of cross-reaction with other carbonic anhydrases (a feature that small molecule inhibitors lack), capacity to internalize, ability to block acidification and retard the tumor growth.

The CA9hu-2 antibody is exceptional due to its binding to the linear epitope in the N-terminal proteoglycan domain of CA IX. After binding to the epitope, the antibody is able to block the attachment of tumor cells to the extracellular matrix, leading to the decrease of metastases. Similarly, to CA9hu-1, CA9hu-2 antibody decreases extracellular acidification, and does not cross-react with other carbonic anhydrases that play important roles in non-pathological condition.

Most importantly, both antibodies exhibit the ability to induce ADCC and ADCP activities, which allows to use them in clinical practice as effective single agents without the need for antibody-drug conjugate.

The humanized antibodies are a new hope in the field of carbonic anhydrases mainly due to their optimal structure preventing undesired HAMA effects. Compared to chimeric G250 (known as RENCAREX® or GIRENTUXIMAB®), humanized antibodies CA9hu-1 and CA9hu-2 show lower non-specific immunogenicity in terms of HAMA response, and higher expected specific efficacy.

In summary, this investigation has demonstrated that CA9hu-1 and CA9hu-2 humanized antibodies are highly specific to hypoxia-induced CA IX cancer biomarker. They are able to interfere with the function of CA IX in tumor biology and are also capable of engaging innate immune effector mechanisms involved in killing tumor cells. These findings provide the supporting rationale for the further preclinical investigation and subsequent clinical development of these humanized antibodies as immunotherapeutic drugs for patients with solid tumors expressing CA IX.

Abbreviations

ADCC: antibody-dependent cellular cytotoxicity

ADPC: antibody-dependent cell-mediated phagocytosis

CA9hu-1;2: carbonic anhydrase 9 humanized -1, 2 antibody

CA: carbonic anhydrase

CA IX: carbonic anhydrase IX

ccRCC: clear cell renal cell carcinomas

CDC: complement dependent cytotoxicity

CDR: complementarity-determining region

EC50: half maximal effective concentration

HAMA: human anti-mouse antibody response

HC: antibody heavy chain

HIF(-1): hypoxia inducible factor (1)

IMGT: ImMunoGeneTics information system

LC: antibody light chain

mAb: monoclonal antibodies

NFAT: nuclear factor of activated T-cells

PG: proteoglycan-like domain

RLU: relative luminescence units

SPR: surface plasmon resonance

TME: tumor microenvironment

TNBC: triple negative breast cancer

VHL: von Hippel-Lindau

V_H: heavy variable domain

V_L: light variable domain

References

1. Harris AL. Hypoxia - A key regulatory factor in tumour growth. Nat Rev Cancer. 2002;2:38–47.

2. Gillies RJ, Brown JS, Anderson ARA, Gatenby RA. Eco-evolutionary causes and consequences of temporal changes in intratumoural blood flow. Nat Rev Cancer. 2018;18:576–85.

3. Ratcliffe PJ. Oxygen sensing and hypoxia signalling pathways in animals: The implications of physiology for cancer. J Physiol. 2013;591:2027–42.

4. Choudhry H, Harris AL. Advances in Hypoxia-Inducible Factor Biology. Cell Metab. 2018;27:281–98.

5. Bensaad K, Harris AL. Hypoxia and metabolism in cancer. Adv Exp Med Biol. 2014;772:1–39.

6. Pastorek J, Pastorekova S, Callebaut I, Mornon JP, Zelnik V, Opavsky R, et al. Cloning and characterization of MN, a human tumor-associated protein with a domain homologous to carbonic anhydrase and a putative helix-loop-helix DNA binding segment. Oncogene. 1994;9:2877–88.

7. Pastorekova S, Gillies RJ. The role of carbonic anhydrase IX in cancer development: links to hypoxia, acidosis, and beyond. Cancer Metastasis Rev. 2019;38:65–77.

8. Wykoff CC, Beasley NJP, Watson PH, Turner KJ, Pastorek J, Sibtain A, et al. Hypoxia-inducible expression of tumor-associated carbonic anhydrases. Cancer Res. 2000;60:7075–83.

9. Opavský R, Pastoreková S, Zelník V, Gibadulinová A, Stanbridge EJ, Závada J, et al. Human MN/CA9 gene, a novel member of the carbonic anhydrase family: Structure and exon to protein domain relationships. Genomics. 1996;33:480–7.

10. Innocenti A, Pastorekova S, Pastorek J, Scozzafava A, Simone G De, Supuran CT. The proteoglycan region of the tumor-associated carbonic anhydrase isoform IX acts as anintrinsic buffer optimizing CO2 hydration at acidic pH values characteristic of solid tumors. Bioorganic Med Chem Lett. 2009;19:5825–8.

11. Mahon BP, Bhatt A, Socorro L, Driscoll JM, Okoh C, Lomelino CL, et al. The Structure of Carbonic Anhydrase IX Is Adapted for Low-pH Catalysis. Biochemistry. 2016;55:4642–53.

12. Mboge MY, Mahon BP, McKenna R, Frost SC. Carbonic anhydrases: Role in pH control and cancer. Metabolites. 2018;8.

13. Becker HM. Carbonic anhydrase IX and acid transport in cancer. Br J Cancer. 2020;122:157–67.

14. Švastová E, Hulíková A, Rafajová M, Zaťovičová M, Gibadulinová A, Casini A, et al. Hypoxia activates the capacity of tumor-associated carbonic anhydrase IX to acidify extracellular pH. FEBS Lett [Internet]. 2004;577:439–45. Available from: http://doi.wiley.com/10.1016/j.febslet.2004.10.043

15. Csaderova L, Debreova M, Radvak P, Stano M, Vrestiakova M, Kopacek J, et al. The effect of carbonic anhydrase IX on focal contacts during cell spreading and migration. Front Physiol [Internet]. 2013;4 OCT. Available from: http://journal.frontiersin.org/article/10.3389/fphys.2013.00271/abstract

16. Betts MJ, Russell RB. Amino Acid Properties and Consequences of Substitutions [Internet]. Chichester, UK: John Wiley & Sons, Ltd; 2003. Available from: http://doi.wiley.com/10.1002/0470867302.ch14

17. Chiche J, Ilc K, Laferrière J, Trottier E, Dayan F, Mazure NM, et al. Hypoxia-inducible carbonic anhydrase IX and XII promote tumor cell growth by counteracting acidosis through the regulation of the intracellular pH. Cancer Res. 2009;69:358–68.

18. Chafe SC, Dedhar S. Carving out its niche: A role for carbonic anhydrase IX in pre-metastatic niche development. Oncoimmunology. 2015;4.

19. Ledaki I, McIntyre A, Wigfield S, Buffa F, McGowan S, Baban D, et al. Carbonic anhydrase IX induction defines a heterogeneous cancer cell response to hypoxia and mediates stem cell-like properties and sensitivity to HDAC inhibition. Oncotarget. 2015;6:19413–27.

20. Noman MZ, Hasmim M, Lequeux A, Xiao M, Duhem C, Chouaib S, et al. Improving Cancer Immunotherapy by Targeting the Hypoxic Tumor Microenvironment: New Opportunities and Challenges. Cells. 2019;8.

21. Jing X, Yang F, Shao C, Wei K, Xie M, Shen H, et al. Role of hypoxia in cancer therapy by regulating the tumor microenvironment. Mol Cancer. 2019;18.

22. Codony VL, Tavassoli M. Hypoxia-induced therapy resistance: Available hypoxia-targeting strategies and current advances in head and neck cancer. Transl Oncol. 2021;14.

23. Wang B, Zhao Q, Zhang Y, Liu Z, Zheng Z, Liu S, et al. Targeting hypoxia in the tumor microenvironment: a potential strategy to improve cancer immunotherapy. J Exp Clin Cancer Res. 2021;40.

24. Pastorek J, Pastorekova S. Hypoxia-induced carbonic anhydrase IX as a target for cancer therapy: From biology to clinical use. Semin Cancer Biol. 2015;31:52–64.

25. Van Kuijk SJA, Yaromina A, Houben R, Niemans R, Lambin P, Dubois LJ. Prognostic significance of carbonic anhydrase IX expression in cancer patients: A meta-analysis. Front Oncol. 2016;6.

26. Zaťovičová M, Tarábková K, Švastová E, Gibadulinová A, Mucha V, Jakubíčková L, et al. Monoclonal antibodies generated in carbonic anhydrase IX-deficient mice recognize different domains of tumour-associated hypoxia-induced carbonic anhydrase IX. J Immunol Methods. 2003;282:117–34.

27. Kabat EA, Wu T Te, Perry HM, Foeller C, Gottesman KS. Sequences of proteins of immunological interest. Anal Biochem. DIANE Publishing; 1984;138:265.

28. Lefranc MP, Pommié C, Ruiz M, Giudicelli V, Foulquier E, Truong L, et al. IMGT unique numbering for immunoglobulin and T cell receptor variable domains and Ig superfamily V-like domains. Dev Comp Immunol. 2003;27:55–77.

29. Ditte P, Dequiedt F, Svastova E, Hulikova A, Ohradanova-Repic A, Zatovicova M, et al. Phosphorylation of carbonic anhydrase IX controls its ability to mediate extracellular acidification in hypoxic tumors.

Cancer Res [Internet]. 2011;71:7558–67. Available from: http://cancerres.aacrjournals.org/cgi/doi/10.1158/0008-5472.CAN-11-2520

30. Zatovicova M, Jelenska L, Hulikova A, Csaderova L, Ditte Z, Ditte P, et al. Carbonic Anhydrase IX as an Anticancer Therapy Target: Preclinical Evaluation of Internalizing Monoclonal Antibody Directed to Catalytic Domain. Curr Pharm Des. 2010;16:3255–63.

31. Almagro JC, Fransson J. Humanization of antibodies. Front Biosci. 2008;13:1619–33.

32. Chung S, Quarmby V, Gao X, Ying Y, Lin L, Reed C, et al. Quantitative evaluation of fucose reducing effects in a humanized antibody on Fcγ receptor binding and antibody-dependent cell-mediated cytotoxicity activities. MAbs. 2012;4:326–40.

33. Zahavi D, Weiner L. Monoclonal Antibodies in Cancer Therapy. Antibodies (Basel). 2020;9:34.

34. Lu RM, Hwang YC, Liu IJ, Lee CC, Tsai HZ, Li HJ, et al. Development of therapeutic antibodies for the treatment of diseases. J Biomed Sci. 2020;27.

35. Shek D, Read SA, Ahlenstiel G, Piatkov I. Pharmacogenetics of anticancer monoclonal antibodies. Cancer Drug Resist. 2019;2:69–81.

36. Mandriota SJ, Turner KJ, Davies DR, Murray PG, Morgan N V., Sowter HM, et al. HIF activation identifies early lesions in VHL kidneys: Evidence for site-specific tumor suppressor function in the nephron. Cancer Cell. 2002;1:459–68.

37. Luiten RM, Coney LR, Fleuren GJ, Warnaar SO, Litvinov S V. Generation of chimeric bispecific G250/anti-CD3 monoclonal antibody, a tool to combat renal cell carcinoma. Br J Cancer. 1996;74:735–44.

38. Luiten RM, Warnaar SO, Schuurman J, Pasmans SGMA, Latour S, Daëron M, et al. Chimeric immunoglobulin E reactive with tumor-associated antigen activates human FcεRI bearing cells. Hum Antibodies. 1997;8:169–80.

39. Oosterwdk E, Ruiter DJ, Hoedemaeker PJ, Pauwels EKJ, Jonas U, Zwartendijk I, et al. Monoclonal antibody G 250 recognizes a determinant present in renal-cell carcinoma and absent from normal kidney. Int J Cancer. 1986;38:489–94.

40. Oosterwijk-Wakka JC, Boerman OC, Mulders PFAM, Oosterwijk E. Application of monoclonal antibody G250 recognizing carbonic anhydrase IX in renal cell carcinoma. Int J Mol Sci. 2013;14:11402–23.

41. Davis ID, Liu Z, Saunders W, Lee FT, Spirkoska V, Hopkins W, et al. A pilot study of monoclonal antibody cG250 and low dose subcutaneous IL-2 in patients with advanced renal cell carcinoma. Cancer Immun. 2007;7.

42. Seidel UJE, Schlegel P, Lang P. Natural killer cell mediated antibody-dependent cellular cytotoxicity in tumor immunotherapy with therapeutic antibodies. Front Immunol. 2013;4.

43. Belldegrun AS, Chamie K, Kloepfer P, Fall B, Bevan P, Störkel S, et al. ARISER: A randomized double blind phase III study to evaluate adjuvant cG250 treatment versus placebo in patients with high-risk ccRCC—Results and implications for adjuvant clinical trials. J Clin Oncol. 2013;31:4507–4507.

44. Xu C, Lo A, Yammanuru A, Tallarico ASC, Brady K, Murakami A, et al. Unique biological properties of catalytic domain directed human anti-CAIX antibodies discovered through phage-display technology. PLoS One. 2010;5.

45. Chang DK, Moniz RJ, Xu Z, Sun J, Signoretti S, Zhu Q, et al. Human anti-CAIX antibodies mediate immune cell inhibition of renal cell carcinoma in vitro and in a humanized mouse model in vivo. Mol Cancer. 2015;14.

46. Petrul HM, Schatz CA, Kopitz CC, Adnane L, McCabe TJ, Trail P, et al. Therapeutic Mechanism and Efficacy of the Antibody–Drug Conjugate BAY 79-4620 Targeting Human Carbonic Anhydrase 9. Mol Cancer Ther [Internet]. 2012;11:340–9. Available from: http://mct.aacrjournals.org/lookup/doi/10.1158/1535-7163.MCT-11-0523

Figures

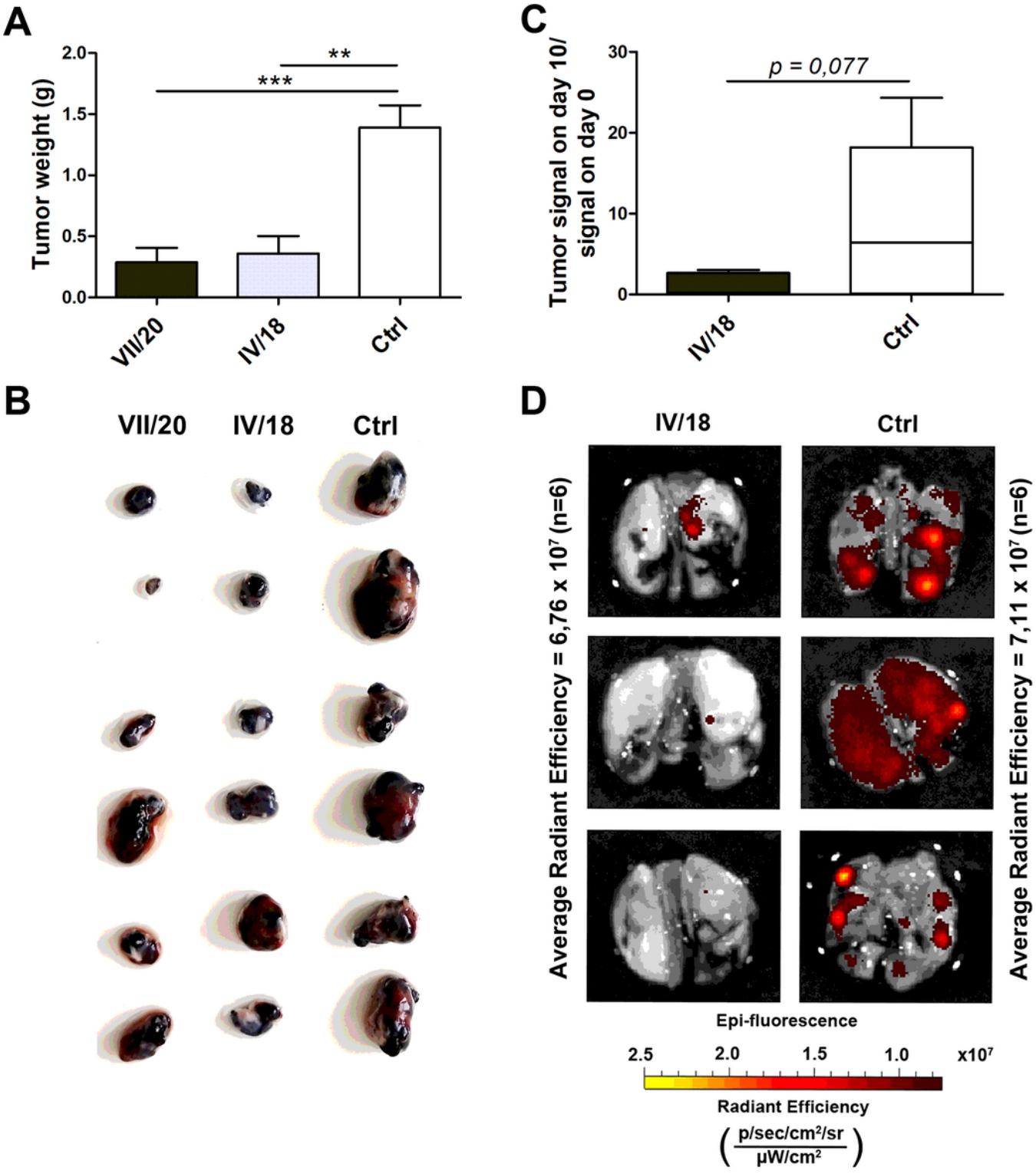

Figure 1

Anti-tumor effect of CA IX-specific mouse monoclonal antibodies in vivo. A and B. Inhibition of tumor growth by antibodies IV/18 and VII/20 on B16-CA IX cells xenografts stably transfected with human CA IX in C57BL/6J mice model. C and D: Inhibition of lung metastases formation of hypoxia pre-incubated HT1080-RFP cells treated by CA IX-specific antibody IV/18 in tail vein colonization assay. Data in the graph represent mean ± standard deviation values. Statistical significance of differences between

antibody treated and non-treated animal was assessed using Student´s t-test (* P< 0.05, ** P< 0.01, *** P<0.001) n=6.

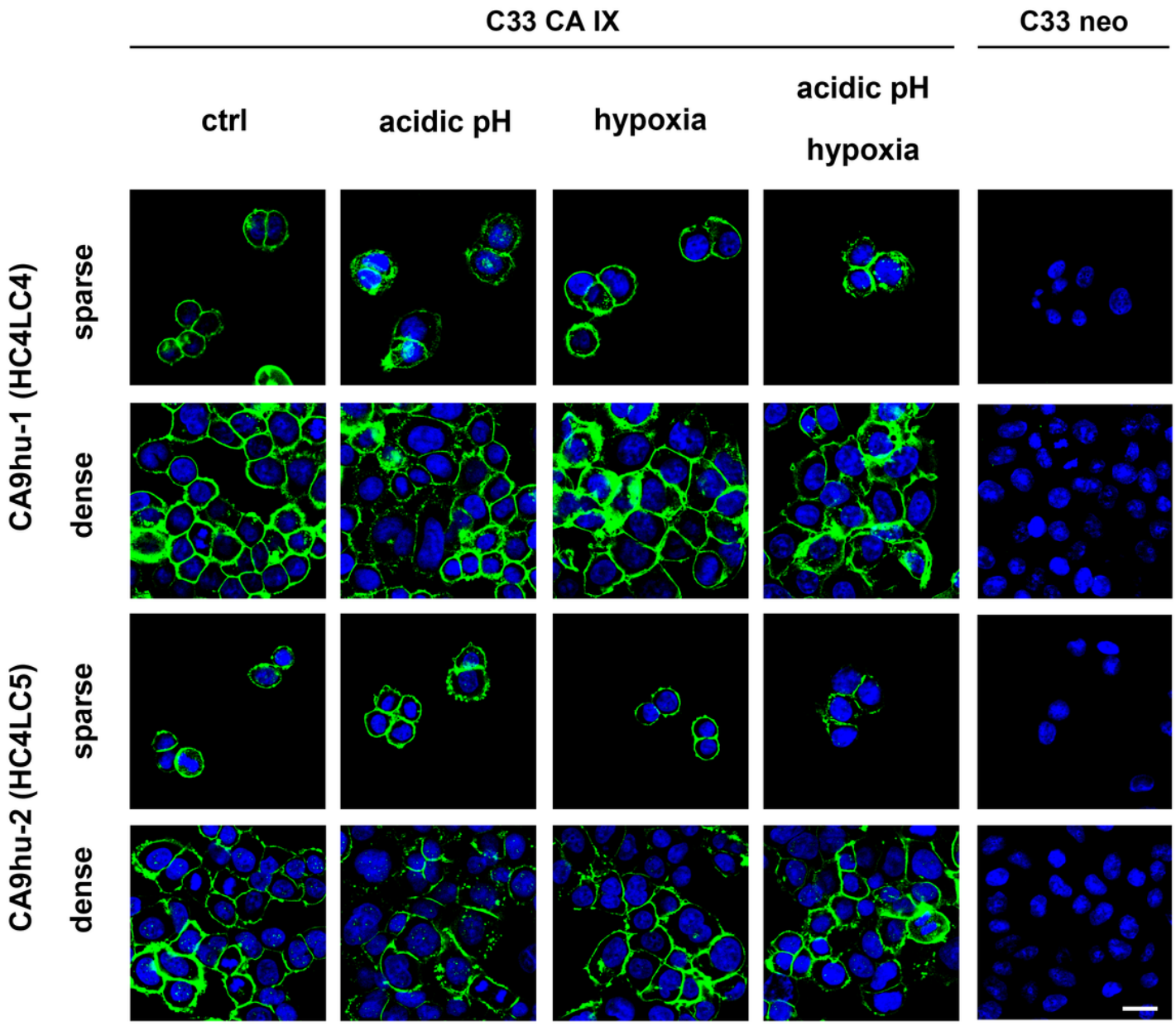

Figure 2

Immunofluorescence detection of CA IX in transfected C33a_CA IX cells. The cells were grown to confluence and incubated with representative monoclonal antibodies in different conditions then fixed by methanol followed by incubation with anti-human Alexa Fluor® 488-conjugated antibody. Both antibodies revealed plasma membrane CA IX-specific staining. Scale bar = 20 μm.

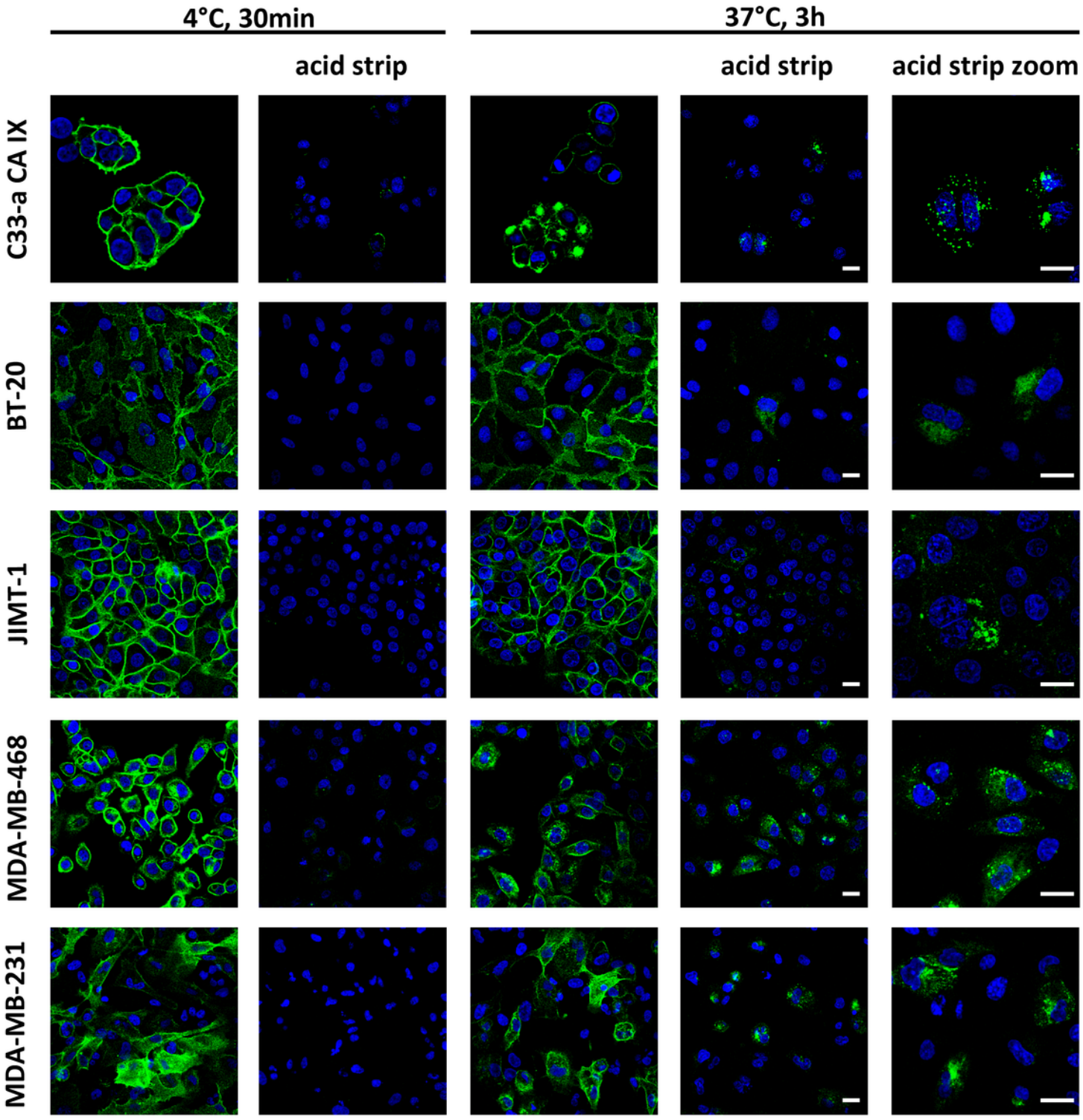

Figure 3

The analysis of humanized antibody variant CA9hu-1(HC4LC4) for its capacity to internalize into cancer cells. Visualization by confocal microscopy revealed punctuated intracellular staining signal after acid strip indicating internalization. Cells were incubated with MAb at 4 °C for 30 min and then in parallel at 4 °C (to prevent internalization) and 37 °C (to trigger internalization) for 3 h. After fixation with methanol,

the cells were stained with anti-human Alexa Fluor® 488-conjugated antibody in order to visualize the MAbs. Acid strip before fixation was used to remove membrane bound antibody. Scale bar = 20 µm.

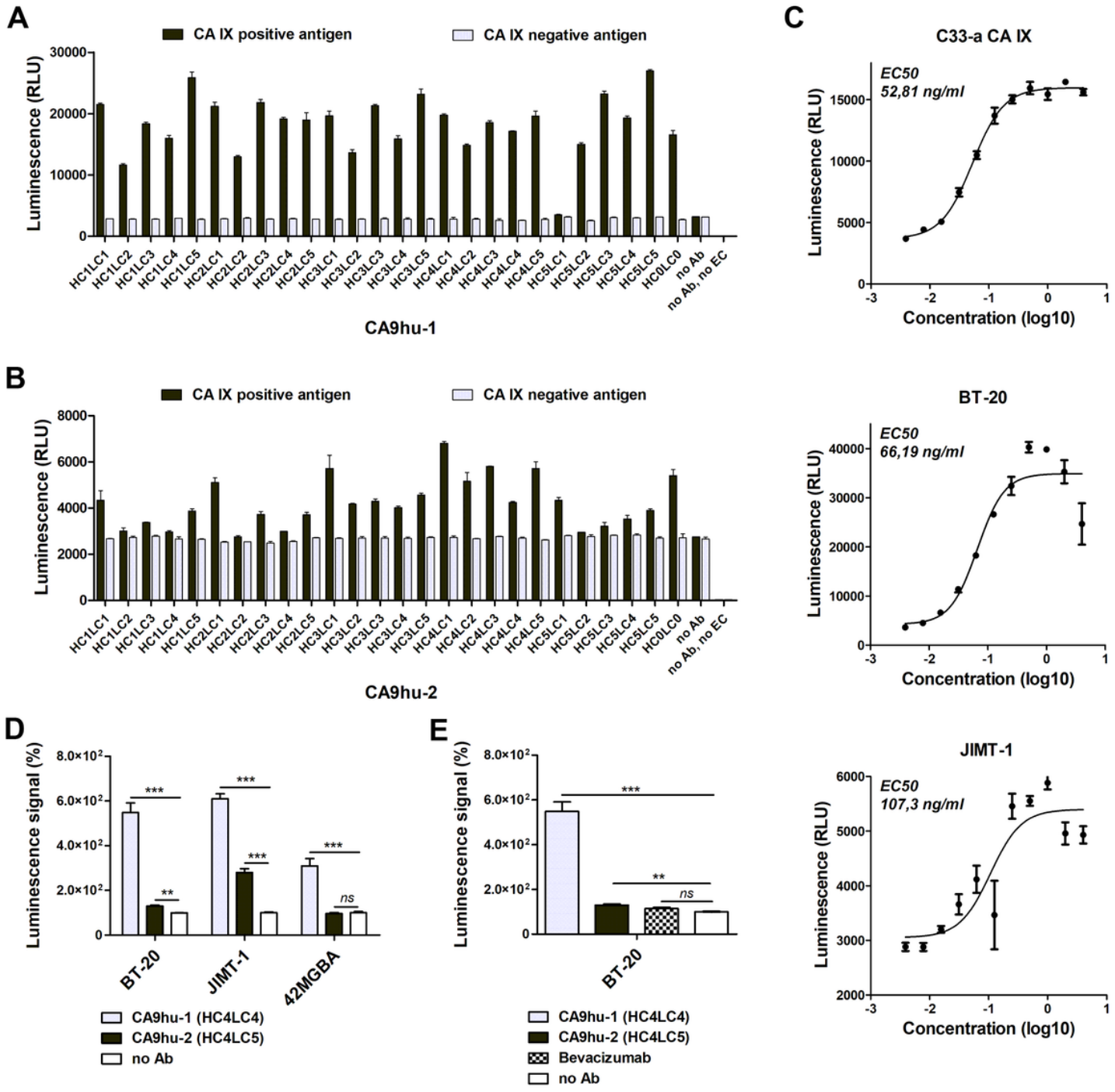

Figure 4

A and B: Graphical representation of ADCC data. CA9hu-1 and CA9hu-2 antibody variants dependent cell-mediated cytotoxicity. Comparison of CA IX-negative versus CA IX-positive target cell line samples, n=2. C: Fit curves determine EC50 of CA9hu-1(HC4LC5) antibody response using GraphPad Prism® software. D: Humanized antibody variants showed high ADCC activity in Reporter ADCC assay (Promega) tested on cells expressing CA IX in hypoxia. The signal of the control was set as 100%. E: Humanized antibody

variants showed high ADCC activity in comparison to irrelevant therapeutic antibody Bevacizumab. Figure 4 clearly shows that humanized antibody variants CA9hu-1 and CA9hu-2 retain the ability to activate ADCC pathway and to mediate cytotoxic effect on target cells expressing CA IX. Data in the graph represent mean ± standard deviation values. Statistical significance of differences was assessed using Student´s t-test (* P< 0.05, ** P< 0.01, *** P<0.001) n=3.

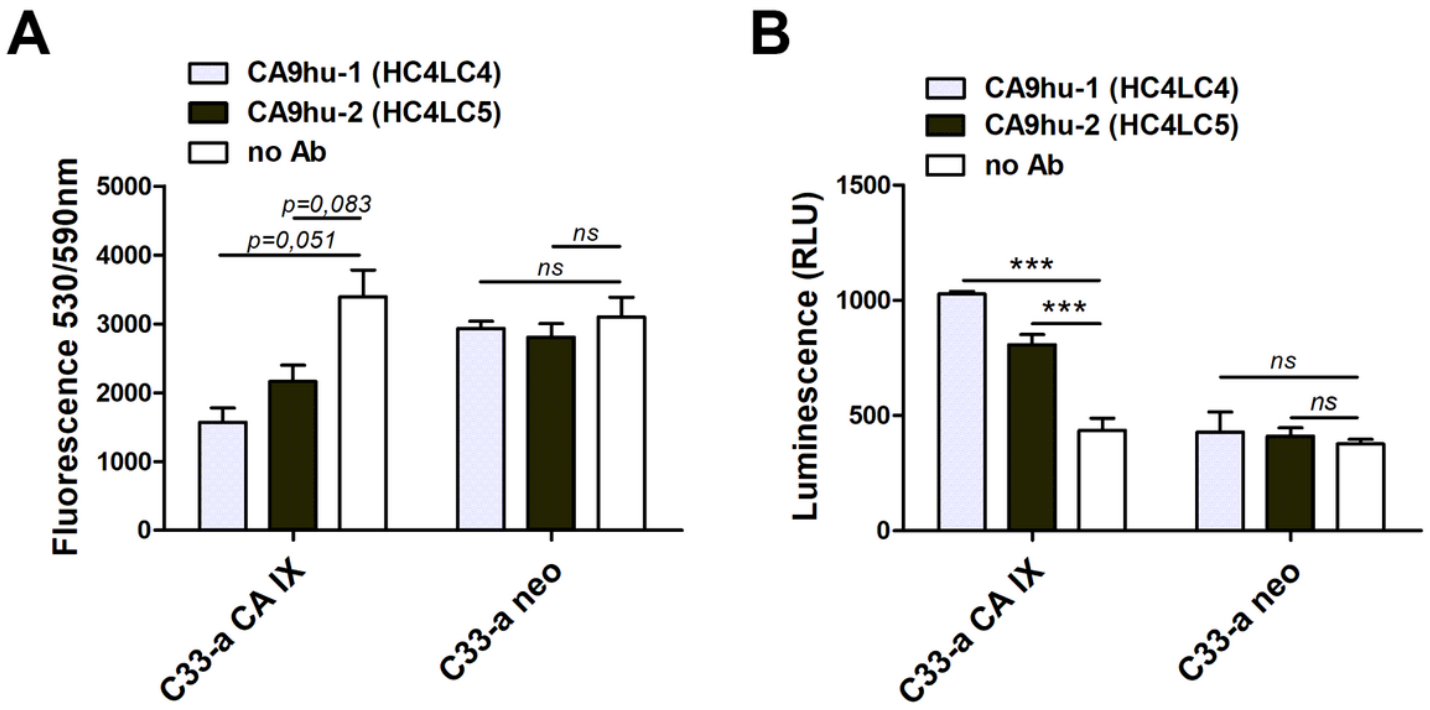

Figure 5

A: The effect of selected humanized antibodies (CA9hu-1(HC4LC4) and CA9hu-2(HC4LC5)) on the viability of analysed cells +/- expressing CA IX (C-33a_CA IX versus C-33a_neo) in the presence of complement determined via Cell Titer Blue Viability Assay. Cancer cells incubated in the absence of humanized antibodies are marked as "no Ab". Data in the graph represent mean ± standard deviation values. Statistical significance was assessed using Student´s t-test (* P< 0.05, ** P< 0.01, *** P<0.001) n=2. B: Graphical representation of ADCP data. CA9hu-1 and CA9hu-2 antibody variants dependent cell-mediated Phagocytosis. Comparison of CA IX-negative versus CA IX-positive target cell line samples. Statistical significance was assessed using Student´s t-test (* P< 0.05, ** P< 0.01, *** P<0.001) n=3.

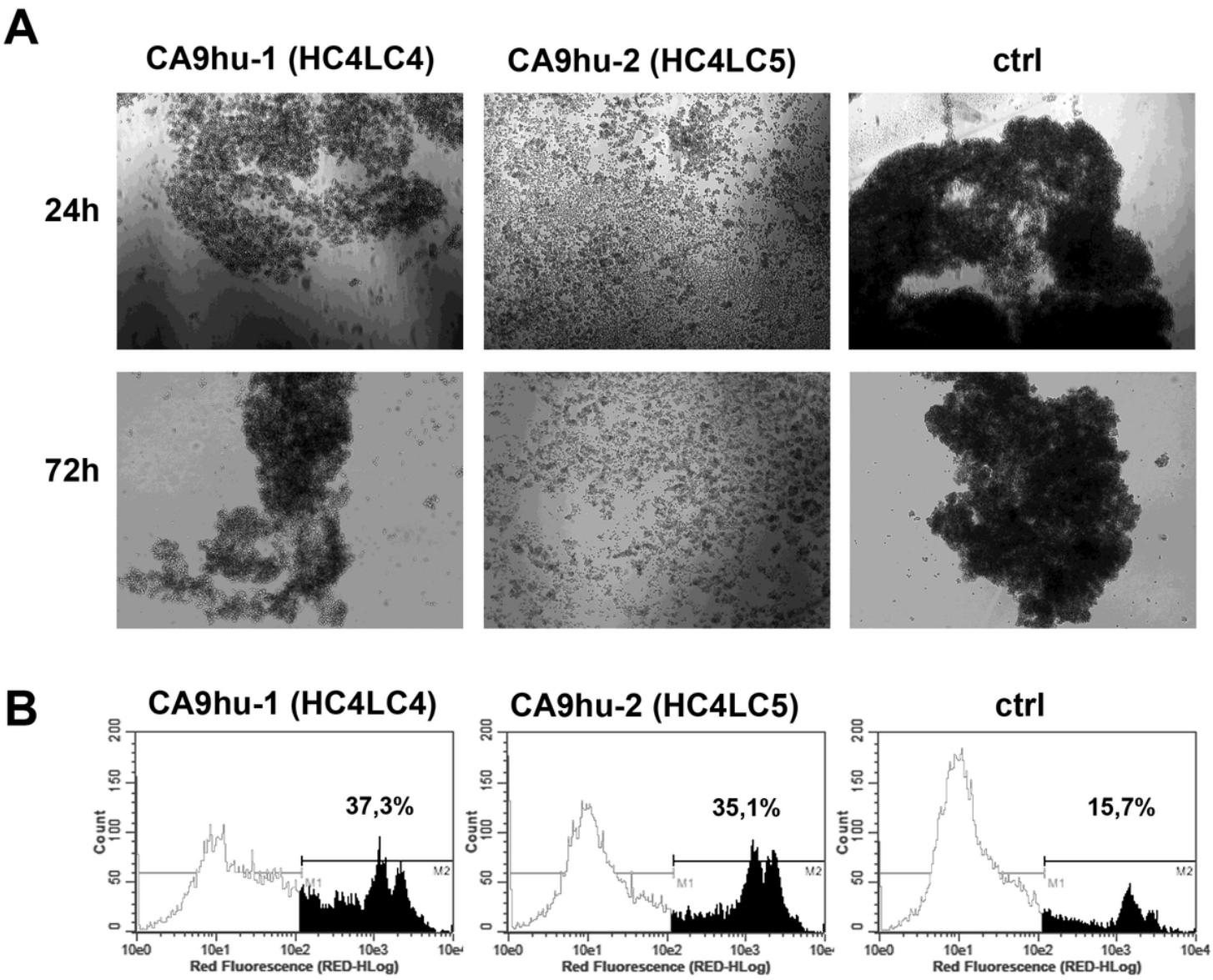

Figure 6

A: Analysis of multicellular aggregation of C-33a_CA IX with humanized antibody CA9hu-1 (HC4LC4) and CA9hu-2 (HC4LC5) after 24 h and 72 h on poly-HEMA coated dishes. C-33a_CA IX cells incubated in the absence of humanized antibody are marked as "negative control". B: Analysis of C-33a_CA IX cells by propidium iodide staining and flow cytometry after 72 h of treatment with humanized CA9hu-1 (HC4LC4) and CA9hu-2 (HC4LC5) antibody. C-33a_CA IX cells incubated in the absence of humanized antibody are marked as "ctrl".

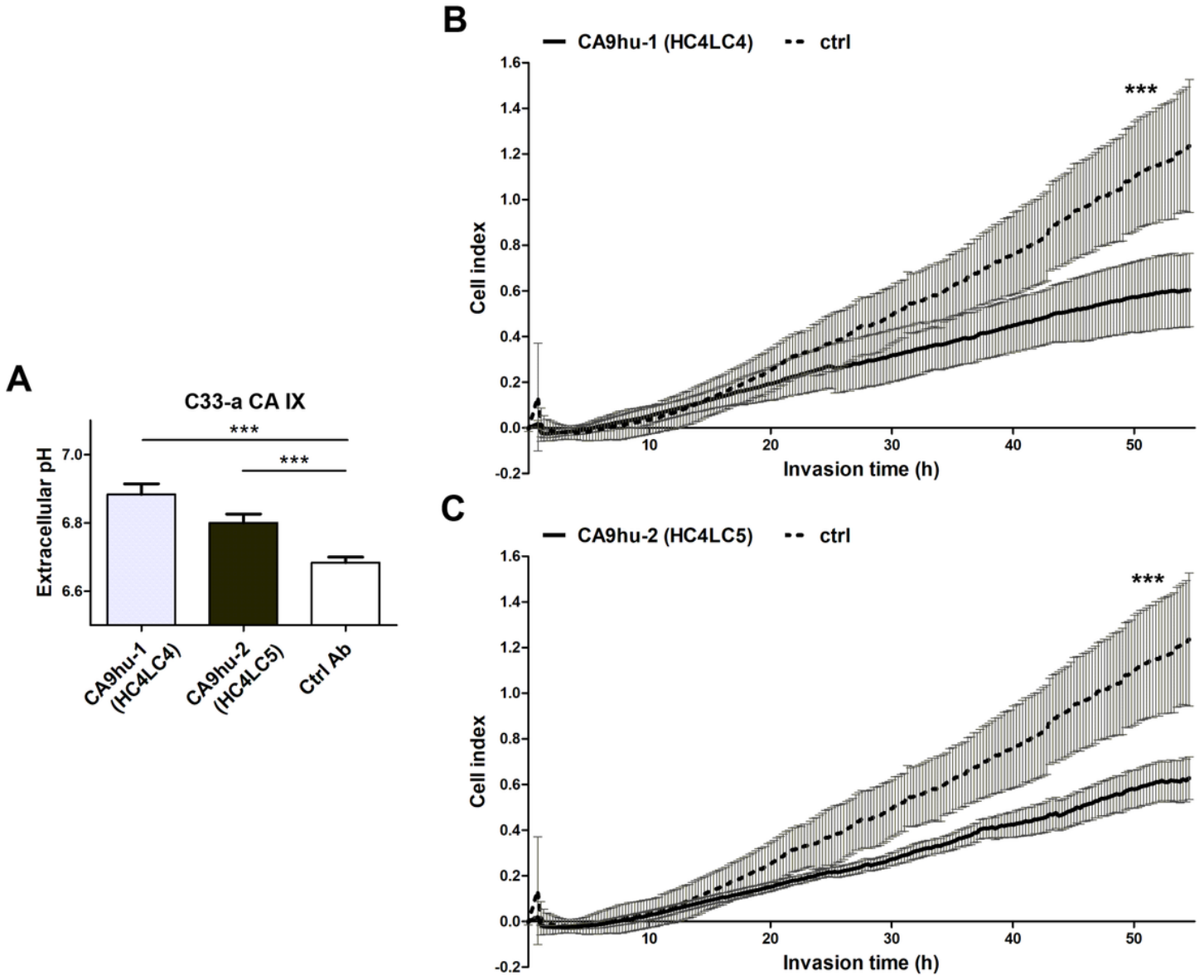

Figure 7

Graphical representation of extracellular pH analysed in C33a_CA IX (A) cells after treatment with CA9hu-1 (HC4LC4) or CA9hu-2 (HC4LC5) for 72 h in hypoxia, n=6. B and C: demonstrate the ability of humanized antibodies to inhibit invasion of cancer cells in comparison with no Ab treatment. Invasion ability of C-33a cells expressing CA IX was significantly reduces after the treatment with both humanized antibody variant. Data in the graph represent mean ± standard deviation values. Statistical significance of differences was assessed using Student´s t-test (* P< 0.05, ** P< 0.01, *** P<0.001) n=6

Supplementary Files

This is a list of supplementary files associated with this preprint. Click to download.

- SUPfig1.tif

- CA9huMAbsMSauthors.docx
- Table1Supplementary.docx